CHAPTER V

STRUCTURAL AND RHEOLOGICAL ASPECT OF MESOPOROUS NANOCRYSTALLINE TiO_2 SYNTHESIZED VIA SOL-GEL PROCESS

Abstract

Mesoporous nanocrystalline titanium dioxide was prepared via the sol-gel technique using titanium glycolate as precursor in 1M HCl solution at various $HCl:H_2O$ ratios. XRD analysis indicates the anatase phase forms at calcination temperatures in the range 600°-800°C. From the average grain sizes, we deduce that the nucleation rate dominates the kinetics at lower temperature, and growth rate becomes the controlling factor at higher temperature for materials prepared at $HCl:H_2O$ ratios of 0.28 and 0.33. At higher volume ratios, the growth rate appears to be the dominant factor at all temperatures. The highest specific surface area (BET) obtained was 125 m^2/g at the $HCl:H_2O$ ratio of 0.28. A small decrease of specific surface area was observed from low to high acid ratio and a substantial decrease from lower to higher temperature. The material calcined at 800°C was found to consist primarily of spherical particles with diameters smaller than 1 μ. Application of the Winter rheological criteria for the gel point indicates that the gelation time increases with increase of the $HCl:H_2O$ volume ratio. The fractal dimension of the critical gel cluster decreases with acid ratio, whereas the gel strength increases with acid ratio. Thus increase of acidity lead to a less dense but stronger network structure.

Keywords: Titanium glycolate, Titania, Rheology, Sol-gel process and Viscoelastic properties

Introduction

Titanium dioxide or titania, TiO_2, is widely used in the field of catalysis, as filters, adsorbents, and catalyst supports [1,2]. The porous anatase form, as compared to the rutile phase, is of greater importance and interest due to its better catalytic properties. Therefore, a key goal is to prepare anatase nanoparticles, with high surface area, uniform particle size and pore structure, and a high anatase-rutile transformation temperature [3].

Sol-gel processing has become one of the most successful techniques for preparing nanocrystalline metallic oxide materials. In general, this method involves the hydrolysis and polycondensation of a metal alkoxide, to ultimately yield hydroxide or oxide under well-specified reaction conditions [4]. The key advantage of preparing metallic oxides by the sol-gel method is the possibility to control their microstructure and homogeneity. To obtain homogeneous nanoscale macromolecular oxide networks via sol-gel processing, control of hydrolysis is essential. The properties and nature of the product are controlled by the particular alkoxide used, the presence of acidic or basic additives, the solvent, and various other processing conditions (e.g. temperature). The calcination temperature is also a key factor, especially for titania preparation. Too low a temperature results in incomplete combustion and too high a temperature causes phase transformation.

Many studies have been directed to prepare titania powder with increased textural and structural stability. For example, Zhang et al.[5] prepared and studied mesoporous nanocrystalline TiO_2 by a sol-gel technique using butanediol mixed with tetrapropylorthotitanate. A surface area of 97 m^2/g was obtained after calcination at 400°C for 2h. Wei *et al.* [6] prepared nanodisperse spherical TiO_2 particles by forced hydrolysis using boiling reflux $Ti(SO_4)_2$ solution in the presence of H_2SO_4. The particle size distribution was in the range 70-100 nm. Sun *et al.* [7] prepared nanosized anatase titania with average grain sizes ranging from 7.4 to 15.2 nm using MOCVD technology to pyrolyze titanium tetrabutoxide in an oxygen containing atmosphere. The smallest average grain size and the highest surface area were obtained at 700°C. Kim *et al.* [8] synthesized ultrafine titania particles by hydrolysis of titanium tetraisopropoxide (TTIP) in the aqueous cores of water/NP-

5/cyclohexane microemulsions. ith increasing calcination temperature from 300° to 700°C, the specific surface area of the TiO_2 particles decreased from 325.6 to 5.9 m^2/g, whereas the average pore radius increased from 1.4 to 25.1 nm. Wu *et al.* [9] synthesized nanocrystalline titanium dioxide using the sol-hydrothermal method with titanium *n*-butoxide (TNB) as precursor, in various acidic media (HCl, HNO_3, H_2SO_4, and CH_3COOH). Nanocrystals of pure rutile with size < 10 nm were obtained at higher HCl concentrations under mild conditions. The propensity of acidic medium for rutile formation is shown as follows: HCl > HNO_3 > H_2SO_4 > HAc. Ding and Liu [15] synthesized nanocrystalline titania powders via sol-gel processing of tetrabutyltitanate in anhydrous ethanol, and showed that HCl-catalyzed hydrolysis favors the formation of the anatase crystal phase.

Knowledge of the evolution in rheological properties during sol-gel processing is a useful guide to the manufacturer when formulating dispersions to optimize the physical properties required in the final product [10]. Thus, in this work, our aims are to synthesize high surface area anatase TiO_2 and to study the rheological properties of titanium glycolate synthesized directly from inexpensive and widely available TiO_2 and ethylene glycol via the Oxide One Pot Synthesis (OOPS) method [11]. We also investigate the influence of the acid concentration used in acid-catalyzed hydrolysis, the effect of calcination temperature on morphology and phase transformation, and gain some insight into the gel mechanism.

Experimental

Materials

Titanium dioxide (surface area 12 m^2/g) was purchased from Sigma-Aldrich Chemical Co. Inc. (USA) and used as received. Ethylene glycol (EG) was purchased from Malinckrodt Baker, Inc. (USA) and purified by fractional distillation at 200°C under nitrogen at atmospheric pressure, before use. Triethylenetetramine (TETA) was purchased from Facai Polytech. Co. Ltd. (Bangkok, Thailand) and distilled under vacuum (0.1 mm/Hg) at 130°C prior to use. Acetonitrile was purchased from Lab-Scan Company Co. Ltd. and purified by distilling over calcium hydride powder.

Instrumental

Fourier transform infrared spectra (FT-IR) were recorded on a VECOR3.0 BRUKER spectrometer with a spectral resolution of 4 cm^{-1} using transparent KBr pellets containing 0.001 g of sample mixed with 0.06 g of KBr. Thermal gravimetric analysis (TGA) was carried out using a Perkin Elmer thermal analysis system with a heating rate of 10°C/min over 30°-800°C temperature range. The mass spectrum was obtained on a Fison Instrument (VG Autospec-ultima 707E) with VG data system, using the positive fast atomic bombardment mode (FAB^+-MS) with glycerol as the matrix, cesium gun as initiator, and cesium iodide (CsI) as a standard for peak calibration. ^{13}C- solid state NMR spectroscopy was performed using a Bruker AVANCE DPX-300 MAS-NMR. Elemental analysis (EA) was carried out on a C/H/N Analyser (Perkin Elmer PE2400 series II).

Preparation of titanium glycolate

The procedure adopted followed previous work [11]. A mixture of TiO_2 (2g, 0.025 mol) and TETA (3.65g, 0.0074 mol) was stirred vigorously in excess EG (25 cm^3) and heated to 200°C for 24 h. The resulting solution was centrifuged to separate the unreacted TiO_2. The excess EG and TETA were removed by vacuum distillation to obtain a crude precipitate. The white solid product was washed with acetonitrile, dried in a vacuum desiccator and characterized using FTIR, ^{13}C-solid state NMR, EA, FAB^+-MS, and TGA.

FTIR: 2927-2855 cm^{-1} (νC-H), 1080 cm^{-1} (νC-O-Ti bond), and 619 cm^{-1} (νTi-O bond). ^{13}C-solid state NMR: two peaks at 74.8 and 79.2 ppm. EA: 28.6% C and 4.8% H. FAB^+-MS: approximately 8.5% of the highest m/e at 169 of $[Ti(OCH_2CH_2O)_2]H^+$, 73% intensity at 94 of $[OTiOCH_2]$ and 63.5% intensity at m/e 45 of $[CH_2CH_2OH]$. TGA: one sharp transition at 340 °C and 46.95% ceramic yield corresponding to $Ti(OCH_2CH_2O)_2$.

Sol-gel processing of titanium glycolate

The hydrolysis of titanium glycolate (0.026 g) was carried out via addition of 160 μL of 1M HCl mixed with distilled water in volume ratios of $HCl:H_2O$ 0.45, 0.39, 0.33, and 0.28. The mixtures were magnetically stirred and heated in a water

bath at 50°C until a clear gel was obtained. The gels were calcined for 2 h at 600°, 700°, and 800°C.

Rheological study of titanium glycolate

Gelation occurs when aggregation of particles or molecules takes place in a liquid, under the action of Van der Waals forces or via the formation of covalent or noncovalent bonds. The process can be conveniently monitored using rheological measurement techniques [13]. The rheometric measurements were conducted using an ARES rheometer with parallel plate geometry, 25 mm in diameter. The storage (G') and loss (G") moduli were determined using oscillatory shear at frequencies in the range 0.2-6.4 rad/s. The strain amplitude was small enough to ensure that all experiments were conducted within the linear viscoelastic region, where G' and G" are independent of the strain amplitude. Titanium glycolate 0.026 g was hydrolyzed at different $HCl:H_2O$ volume ratios of 0.45, 0.39, 0.33 or 0.28. The hydrolysis temperature was selected to be 30°C. The mixtures were stirred until homogeneous before being transferred to the rheometer.

Characterization of calcined materials

Crystallinity and average grain sizes were characterized using a D/MAX-2200H Rigaku diffractometer with CuKα radiation on specimens prepared by packing sample powder into a glass holder. The diffracted intensity was measured by step scanning in the 2θ range between 5° to 90°. Specific surface area, nitrogen adsorption-desorption, and pore size distribution were determined using an Autosorp-1 gas sorption system (Quantachrome Corporation) via the Brunauer-Emmett-Teller (BET) method. A gaseous mixture of nitrogen and helium was allowed to flow through the analyzer at a constant rate of 30 cc/min. Nitrogen was used to calibrate the analyzer, and also as the adsorbate at liquid nitrogen temperature. The samples were throughly outgassed for 2h at 150°C, prior to exposure to the adsorbent gas. Material morphology was observed using a JEOL 5200-2AE(MP 15152001) scanning electron microscope. Samples were prepared for SEM analysis by attachment to aluminum stubs, after pyrolysis at 800°C. Prior to analysis, the specimens were dried in a vacuum oven at 70°C for 5 h followed by

coating with gold via vapor deposition. Micrographs of the pyrolyzed sample surfaces were obtained at x10,000 magnification.

Results and discussion

The investigation of the hydrolysis reaction of titanium glycolate precursor using FTIR is illustrated in figure1. The spectra show an increase in the peak intensity of Ti-O-Ti stretching at approximately 500-800 cm^{-1} due to hydrolysis of the precursor. The peak at 1000-1100 cm^{-1}, corresponding to C-O stretching of ethylene glycol also increases, reflecting the production of ethylene glycol during the hydrolysis reaction. In the case of higher acid ratio (0.45), the degree of crosslinking is greater than those obtained from the hydrolysis in lower acid ratios. The acid can act as a catalyst to hydrolyze the alkoxide by protonating the ethoxy ligands during hydrolysis. Thus, the elimination of the protonated ethoxy ligand leaving group is no longer the rate limiting step, and, as a result, the hydrolysis occurs more rapidly.

Calcination is a treatment commonly used to improve the crystallinity of TiO_2 powder. When TiO_2 is calcined at higher temperature, a transformation to rutile phase usually occurs [13] and comprises anatase, rutile, and brookite. XRD patterns (Fig.2) show the phase transformations encountered when titanium glycolate precursor is calcined at temperatures in the range 300°-1100°C. Amorphous material is obtained at the lowest temperature (300°C) whereas at 500°C broader anatase peaks appear. As the calcination temperature increases, the intensity of anatase peaks becomes stronger and well resolved. However, if the calcination temperature is increased to 900°C, small rutile peaks are found, indicating the onset of the transformation to rutile.

The synthesis procedure was changed to obtain porous anatase for better catalytic properties. Specimens obtained via the sol-gel process at different volume ratios of $HCl:H_2O$, viz. 0.45, 0.39, 0.33, and 0.28, were subjected to calcination at 600°, 700°, and 800°C, to obtain porous anatase titania[3]. Fig. 3 shows the XRD patterns of anatase formation in a specimen at the $HCl:H_2O$ volume ratio of 0.28. Our results indicate that the synthesized anatase is stable up to calcination temperatures of 800°C, which is a little higher than previous studies, which report the transformation of anatase to rutile in the range of 600°-700°C [7, 13, 14].

As can be seen in Fig. 4, at 0.28 and 0.33 ratios, the average grain size decreases significantly from 600°C (18.8 and 17.1 nm) to 700°C (13.9 and 14.2 nm) and then increases substantially again at 800°C (31.3 and 29.8 nm). These results are reminiscent of observations by Sun et al [7] of the temperature dependence of grain sizes of anatase produced by the MOCVD method. The size variation was interpreted in terms of the rate of particle growth relative to the rate of particle nucleation. Use of elevated temperatures accelerates not only the nucleation rate but also the particle growth rate. For acid:water ratios of 0.28 and 0.33, at lower temperatures, the nucleation rate is dominant, whereas the growth rate becomes the controlling factor at higher temperature. Acid:water ratios of 0.39 and 0.45 ratios show a slightly different pattern, in which grain size increases mildly between 600 °C and 700 °C, and then more dramatically at 800°C, suggest that the growth rate is dominant at all temperatures.

Coincidentally, the nitrogen adsorption-desorption isotherm of the material obtained at 0.28 $HCl:H_2O$ volume ratio and calcined at 600 °C for 2h indicates a mesoporous structure, as seen in figure 5(a). The isotherm is of type IV, characteristic of mesoporous material. The hysteresis loop exhibited by the specimen is mainly of type H2. The pore size distribution in figure 5(b) shows a major porosity in the range of 4-18 nm. To confirm an increase in crystallinity as temperature increases, specific surface area measurements were carried out and, as expected, we find that the higher the calcined temperature, the lower the specific surface area. The powders become dense and predominantly nonporous when the precursor is calcined at 800°C. It is known [3] that a lower acid concentration results in a higher specific surface area due to an increasing in the cross-linking level. This is consistent with our observation that the specific surface area decreases in the following order; 0.28 > 0.33 > 0.39 > 0.45 (Table 1). It can be concluded that sol-gel processing indeed provides a larger specific surface area which decreases with increasing calcinations temperature and acid concentration.

The particle morphology of the samples obtained using a $HCl:H_2O$ ratio of 0.33, when calcined at temperatures in the range 600°-800°C, is shown in Fig. 6. At the lowest two temperatures, Figs. 6(a) and 6(b), the material consists of particles of

large size, whereas the micrograph (Fig.6c) of the material calcined at 800°C shows a finely-divided morphology in the anatase form consisting of spherical particles approximately 1 μm in size.

Viscoelastic studies of the four different gelling systems (volume ratio 0.28, 0.33, 0.39, and 0.45 of $HCl:H_2O$, respectively) were carried out using the criteria proposed by Winter and Chambon [15] to determine the gel point, as the gelation time where a frequency-independent value of tanδ in observed. The variation in the frequency-dependence of tanδ with gelation time is shown in fig.7, and indeed indicates tanδ become frequency independent at a particular gelation time. The shortest gelation time was observed for the system at 0.28 volume ratio (365s) and the longest gelation time for the system of 0.45 volume ratio (870s). An alternative method [16] to determine the gel point is to plot the time evolution of the apparent viscoelastic exponents n' and n" obtained from the frequency-dependence of the modulus ($G' \propto \omega^{n'}$, $G'' \propto \omega^{n''}$), as shown in fig.8 for the system at 0.45 volume ratio. The gel point is identified as the time where a crossover n'=n"=n is observed. The points of intersection (t_{gel}) are found to be the same as those deduced from the plot of tanδ versus time.

It is important to note that these gelling systems are highly elastic even well before the gel point, as evidenced by the fact that $\tan\delta << 1$. Also, the system rheology evolves relatively slowly in the vicinity of the gel point, as seen by plotting the frequency dependence of G' (Pa), G" (Pa) at pregel .stage, gel point, and postgel stage, shown in figure9. The data are shifted horizontally by a factor B. A similar trend is observed for all systems in that G' is higher than G", i.e. elastic behavior predominates before as well as after the gel point. We attribute this behavior to the fact that we are dealing with a concentrated colloidal dispersion, which is converted to a gel by hydrolysis from the outer surfaces of the colloidal particles. Despite this heterogeneous structure, at the gel point, the systems fulfil the Winter criteria that $n'=n''=n_{gel}$, and $\tan\delta = \tan(n_{gel}\pi/2)$ are superimposed [15-19]. The viscoelastic exponent n_{gel} of the system as shown in table2 has its highest value at 0.45 volume acid ratio and the value decreases as the volume acid ratio decreases. Figure 10 shows the effect of $HCl:H_2O$ volume ratio on the gel strength parameter, S, evaluated

from the relationship [16-19] $G'(\omega) = \Gamma(1-n)\cos(n\pi/2)S\omega^n$ where $\Gamma(1-n)$ is the Legendre Γ function. It is evident that the gel strength increases with increasing acid ratio and reaches its highest value acid ratio = 0.39, then decreases slightly. Thus at low acid ratio, the critical gel cluster is relatively weak, at high acid ratio it is stronger.

According to the model of Muthukumar [20] the fractal dimension of the critical gel cluster can be obtained from the viscoelastic exponent n as $n = d(d+2-2d_f)/2(d+2-d_f)$ where d = spatial dimension = 3. The effect of acid ratio on the fractal dimension of incipient gel is shown in fig.11 and table2. The fractal dimension decreases with increasing the acid ratio. A lower fractal dimension mean that the molecular weight grows slower with radius, i.e. $M \sim R^{d_f}$. Thus the critical gel at high acid ratio has a more open structure than at low acid ratio. This is somewhat surprising since we expect the cross-link density to be higher at higher acid ratio. Again we attribute this result to the heterogeneous character of the system at the gel point. The particles which comprise the gel network at low acid ratio are less hydrated and hence more dense than those at higher acid ratio.

Figure12 shows the frequency dependence of the dynamic viscosity at pregel stage, gel point, and postgel stage. Consistent with the highly elastic behavior evident in figure9, at all stages $\eta^*(\omega)$ exhibits power law frequency dependence with an exponent at the gel point of n-1. The time dependence of the complex viscosity at low frequency (ω = 0.4 rad/s) is illustrated in figure 13.The location of the gel point for each system as determined by the Winter criteria (16-19) are indicated by arrows. At low acid ratio, the viscosity is initially high but approaches an asymptotic value which is relatively low. At high acid ratio, the viscosity is initially low but reaches a high asymptotic value. Thus, the gel strength and asymptotic complex viscosity are self-consistent and indicate that the gel becomes stronger under high acidity conditions. We interpret these results as indicating that at low acid, the precursor particles are poorly hydrated and form a more heterogeneous weak gel structure. At high acid, the particles are well solvated and form a less heterogeneous (more open) yet stronger network.

Conclusions

Anatase TiO_2 nanoparticles were successfully prepared by sol-gel technology, using inexpensive and moisture-stable titanium glycolate as precursor in 1M HCl solution. The calcination temperature and the $HCl:H_2O$ volume ratio has a substantial influence on the surface area, phase transformation, and morphology of the products. Anatase titania is produced at calcination temperatures in the range 600 °C to 800 °C, above which transformation to rutile occurs. Increase of temperature results in anatase of higher crystallinity but lower specific surface area, and induces a morphological change from large irregular agglomerates to more homogeneous particles of spherical shape. From XRD measurements of average grain sizes, we deduce that nucleation rate dominates the kinetics at low temperatures, and growth rate becomes the controlling factor at high temperature and low $HCl:H_2O$ ratios. Increase of $HCl:H_2O$ ratio results in a small but significant decrease in porosity. The highest specific surface area 125 m^2/g is obtained at lowest $HCl:H_2O$ ratio 0.28 and lowest calcination temperature (600°C). From rheological analysis, as evaluated by the Winter criteria, the gelation time increases with increase of $HCl:H_2O$ volume ratio. The fractal dimension determined from the frequency scaling exponent of the modulus at the gel point indicates a denses critical gel structure at low acid ratio. However the complex viscosity and gel strength increase as a function of acid ratio. We interpret this behavior as indicative that, at low acidity, the gel is composed of poorly hydrated particles forming a dense but weak structure.Increased acidity increases hydration and cross-link density leading to a more open and stronger gel network.

Acknowledgements

This research work is supported by the Postgraduate Education and Research Program in Petroleum and Petrochemical Technology (ADB) Fund, Ratchadapisakesompoch Fund, Chulalongkorn University and the Thailand Research Fund (TRF).

References

1. J. Yang, S. Mei, J.M. Ferriera, Mat. Sci. Eng. C-Biomim 15 (2001) 183.
2. H. kominami, M. kohno, Y. Takada, M. Inoue, T. Inui, Y. Kera, Ind. Eng. Chem. Res. 38 (1999) 3931.
3. K.M.S. Khalil, T. Baird, M.I. Zaki, A.A. El-Samahy, A.M. Awad, Colloid Surface A 132 (1998) 31.
4. K.M.S. Khalil, M.I. Zaki, Powder Technol. 120 (2001) 256.
5. Y. Zhang, A. Weidenkaff, A. Reller, Mater. Lett. 54 (2002) 375.
6. Y. Wei, R. Wu, Y. Zhang, Mater. Lett. 41 (1999) 101.
7. Y. Sun, A. Li, M. Qi, L. Zhang, X. Yao, Mat. Sci. Eng. B86 (2001) 185.
8. E.J. Kim, S.H. Hahn, Mater. Lett. 49 (2001) 244.
9. M. Wu, G. Lin, D. Chen, G. Wang, D. He, S. Feng, R. Xu, Chem. Mater. 14 (2002) 1974.
10. Kao, S.N. Bhattacharya, J. Rheol. 42 (1998) 493.
11. N. Phonthammachai, T. Chairassameewong, E. Gulari, A.M. Jamieson, S. Wongkasemjit, J. Met. Mat. Min. 12 (2002) 23.
12. Q. Zhang, L. Gao, J. Gao, Appl. Catal. B-Solid 26 (2000) 207.
13. Y. Zhang, A. Weidenkaff, A. Reller, Mater. Lett. 54 (2002) 375.
14. J. Zhao, Z. Wang, L. Wang, H. Yang, M. Zhao, Mater. Chem. Phys. 63 (2000) 9.
15. H.H. Winter, F. Chambon, J. Rheol. 30 (1986) 367.
16. A.L. Kjoniksen, B. Nystrom, Macromolecules 29 (1996) 5215.
17. M. Jokinen, E. Gyorvary, J.B. Rosenholm, Colloid Surface A 141 (1998) 205.
18. B. Nystrom, A.L. Kjonoksen, B. Lindman, Langmuir 12 (1996) 3233.
19. W. Charoenpanijkarn, M. Suwankruhasn, B. Kesapabutr, S. Wongkasemjit, A.M. Jamieson, Eur. Polym. J. 37 (2001) 1441.
20. Muthukumar, M, Macromolecules 22 (1989) 4656.

Table 5.1 BET surface area (S_{BET}, m^2/g) of titania at various HCl:H_2O volume ratios and calcinations temperature

Temperature (°C)	Surface area (m^2/g)			
	0.28	0.33	0.39	0.45
600	125	111	107	105
700	60	59	55	50
800	20	18	17	15

* Surface area of the starting material TiO_2 = 20 m^2/g

Table 5.2 Summary of viscoelastic exponent, fractal dimension, and gelation time(s) at various HCl:H_2O volume ratios

Acid ratio	n	d_f	Gelation time (s)
0.28	0.05	2.46	365
0.33	0.07	2.44	428
0.39	0.19	2.33	647
0.45	0.20	2.32	870

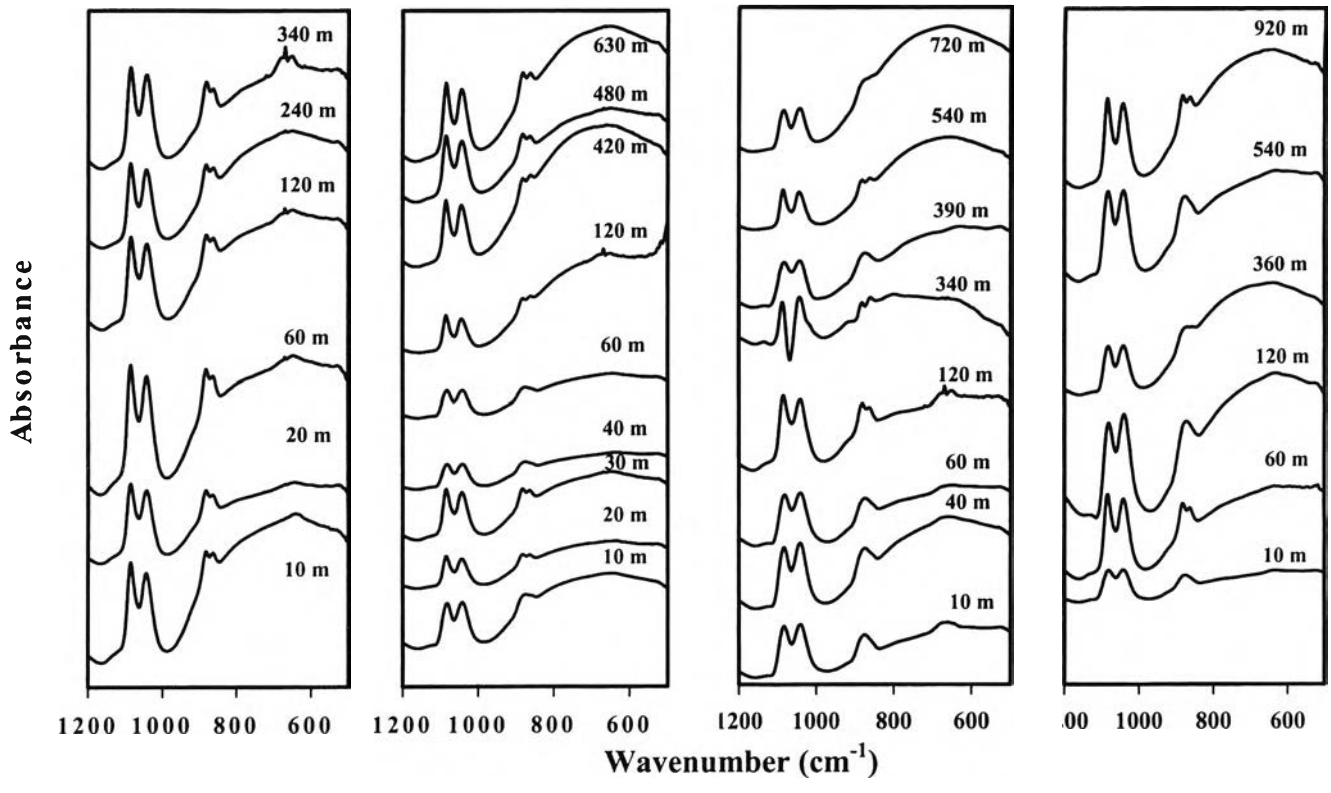

Figure 5.1 The FT-IR spectra of titania gel at HCl:H_2O volume ratio of a.) 0.28, b.) 0.33, c.) 0.39 and d.) 0.45.

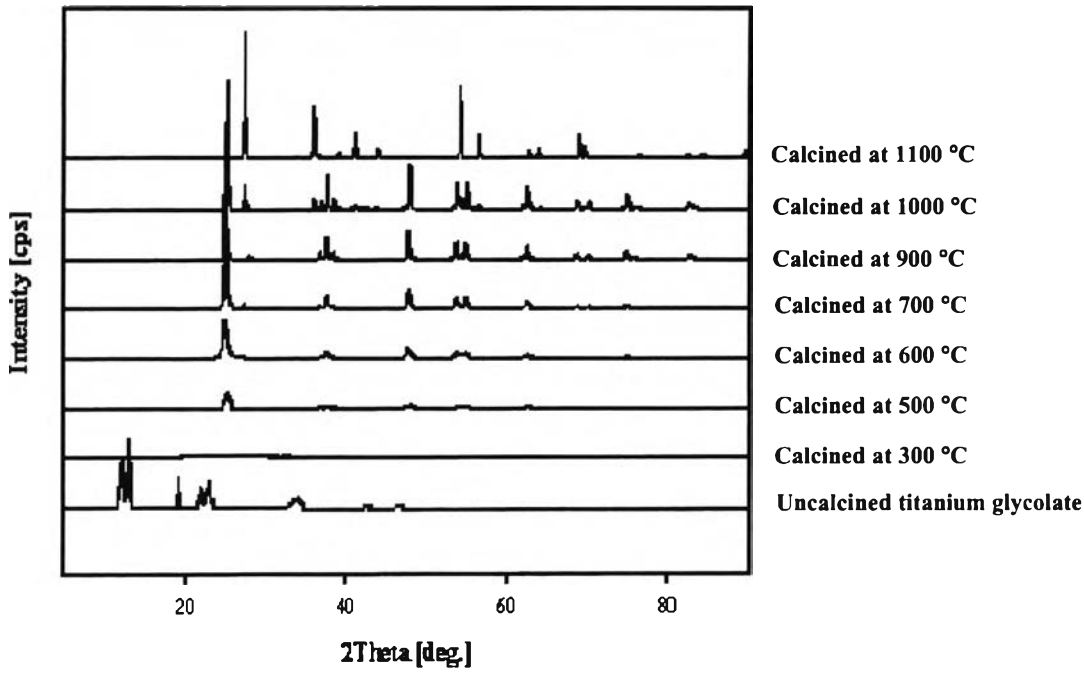

Figure 5.2 XRD patterns of uncalcined and calcined titanium glycolate precursor at different temperatures.

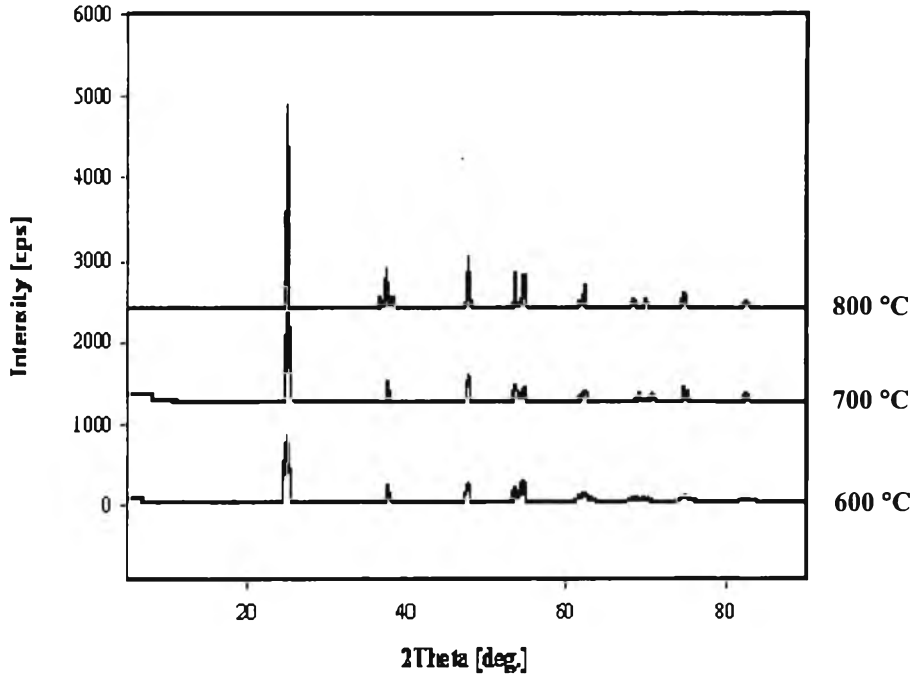

Figure 5.3 XRD pattern of titania gel using the HCl:H_2O volume ratio of 0.28 calcined at a.) 600°, b). 700° and c). 800°C.

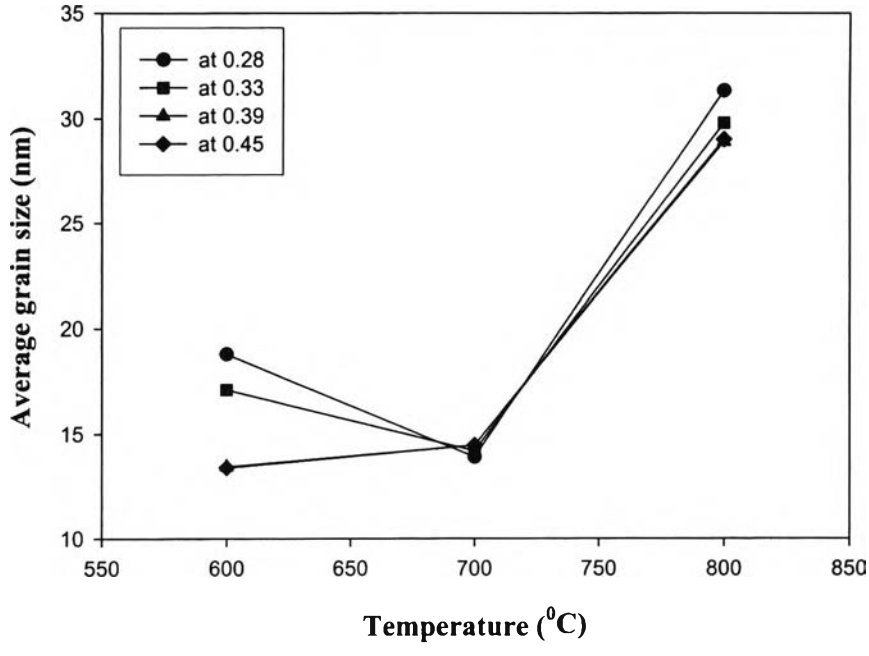

Figure 5.4 The average grain sizes of the particles prepared at different volume ratios of HCl:H_2O (0.28, 0.33, 0.39, 0.45, respectively) and different calcination temperatures (600°, 700° and 800°C).

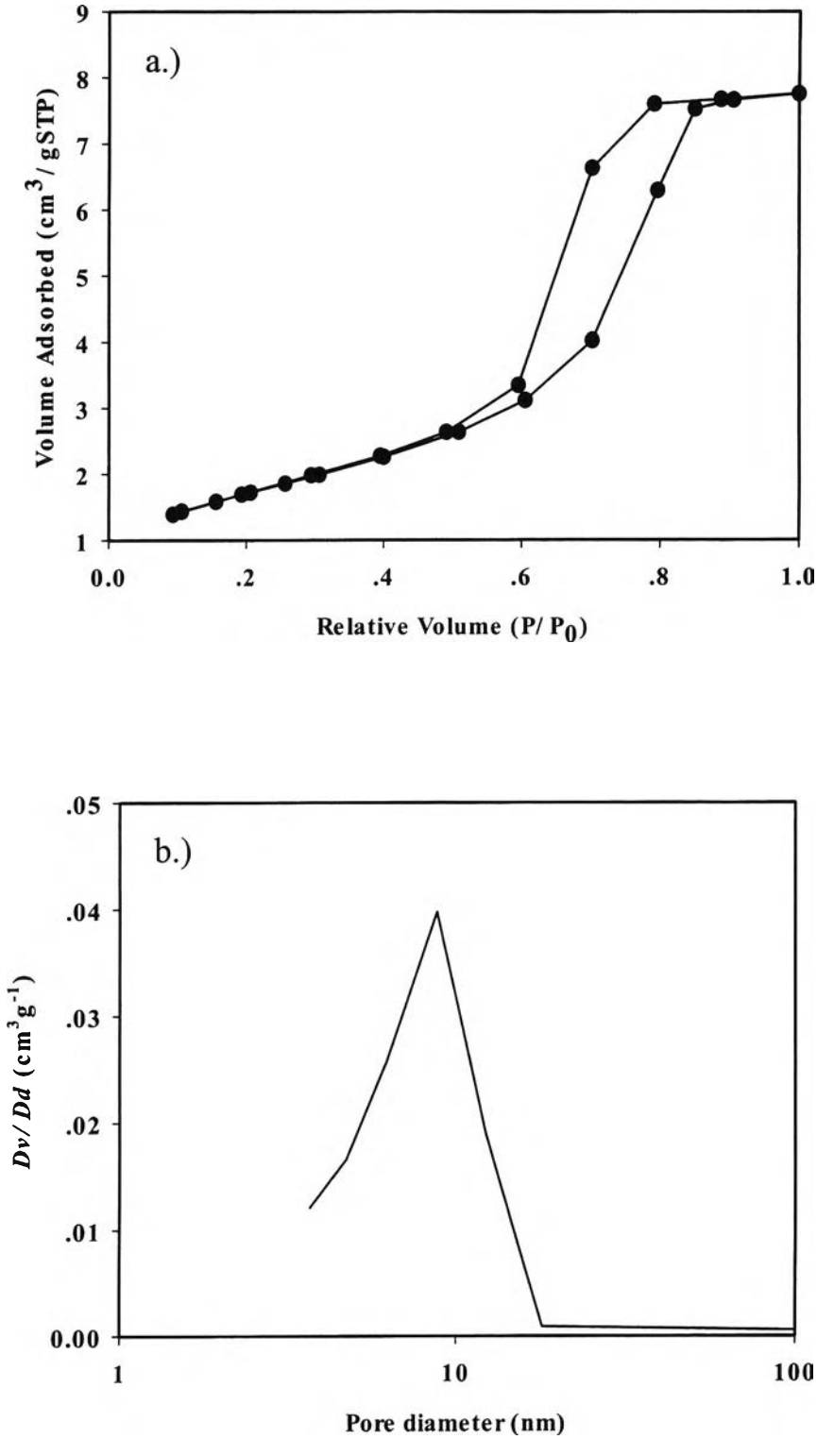

Figure 5.5 The nitrogen adsorption-desorption isoterm for mesoporous titania (a.) and Pore size distribution (b.) for the material obtained from 0.28 HCl:H_2O volume ratio and calcined at 600°C.

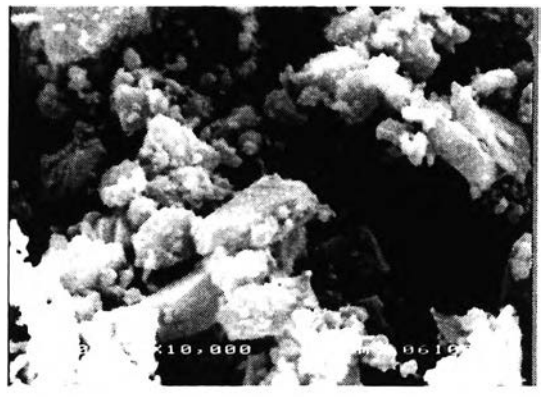

a.)

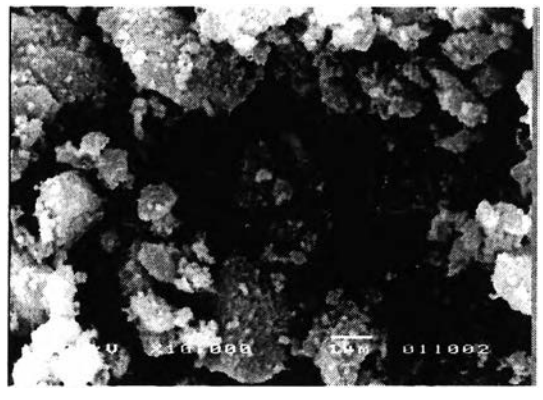

b.)

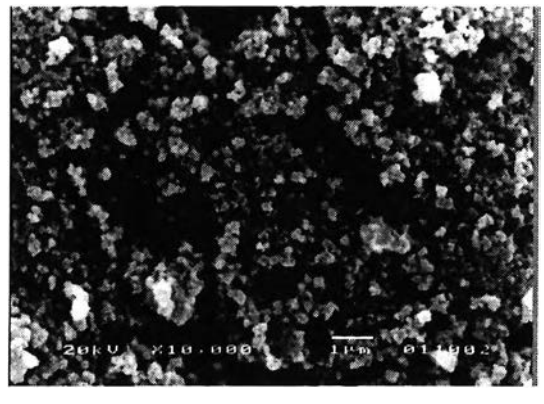

c.)

Figure 5.6 SEM micrograph for titania powder at volume ratio 0.33 of HCl:H_2O calcined at a.) 600°, b.) 700° and c.) 800°C.

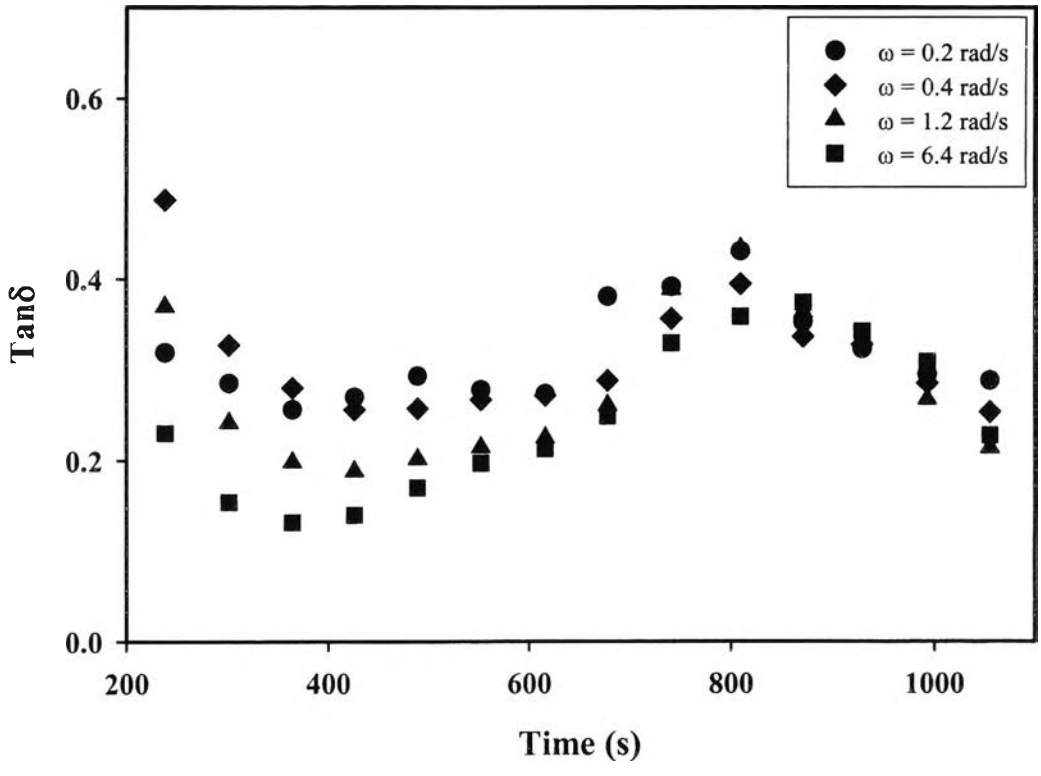

Figure 5.7 The plots of tanδ with time(s) at HCl:H_2O volume ratio of 0.45.

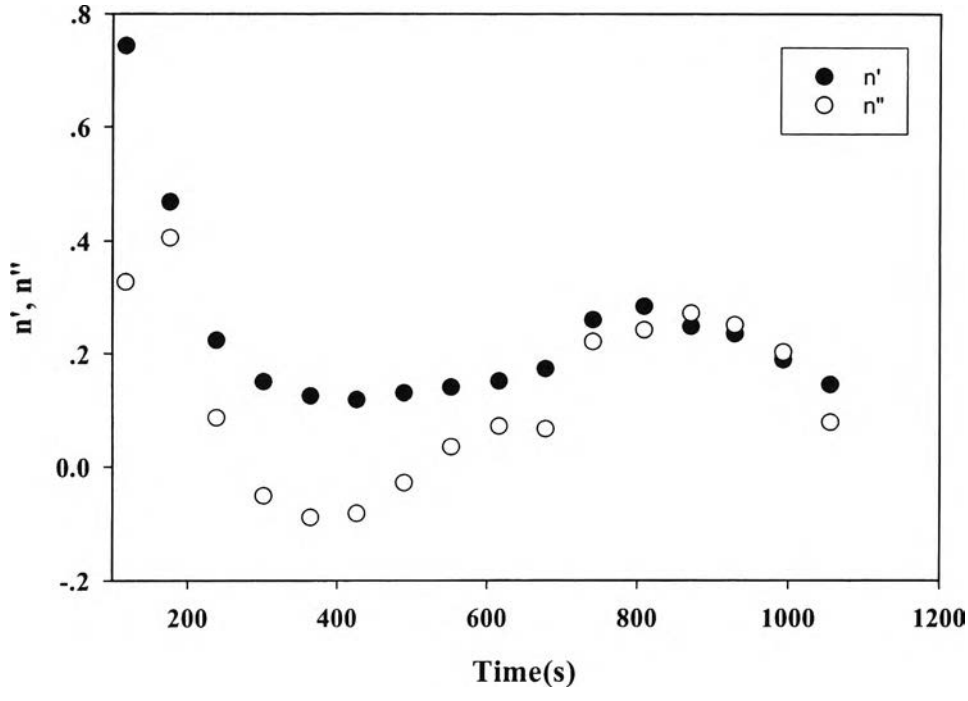

Figure 5.8 The plot of the apparent exponents, the storage moduli (n') and the loss moduli (n") during the course of gelation for the 0.45 acid ratio.

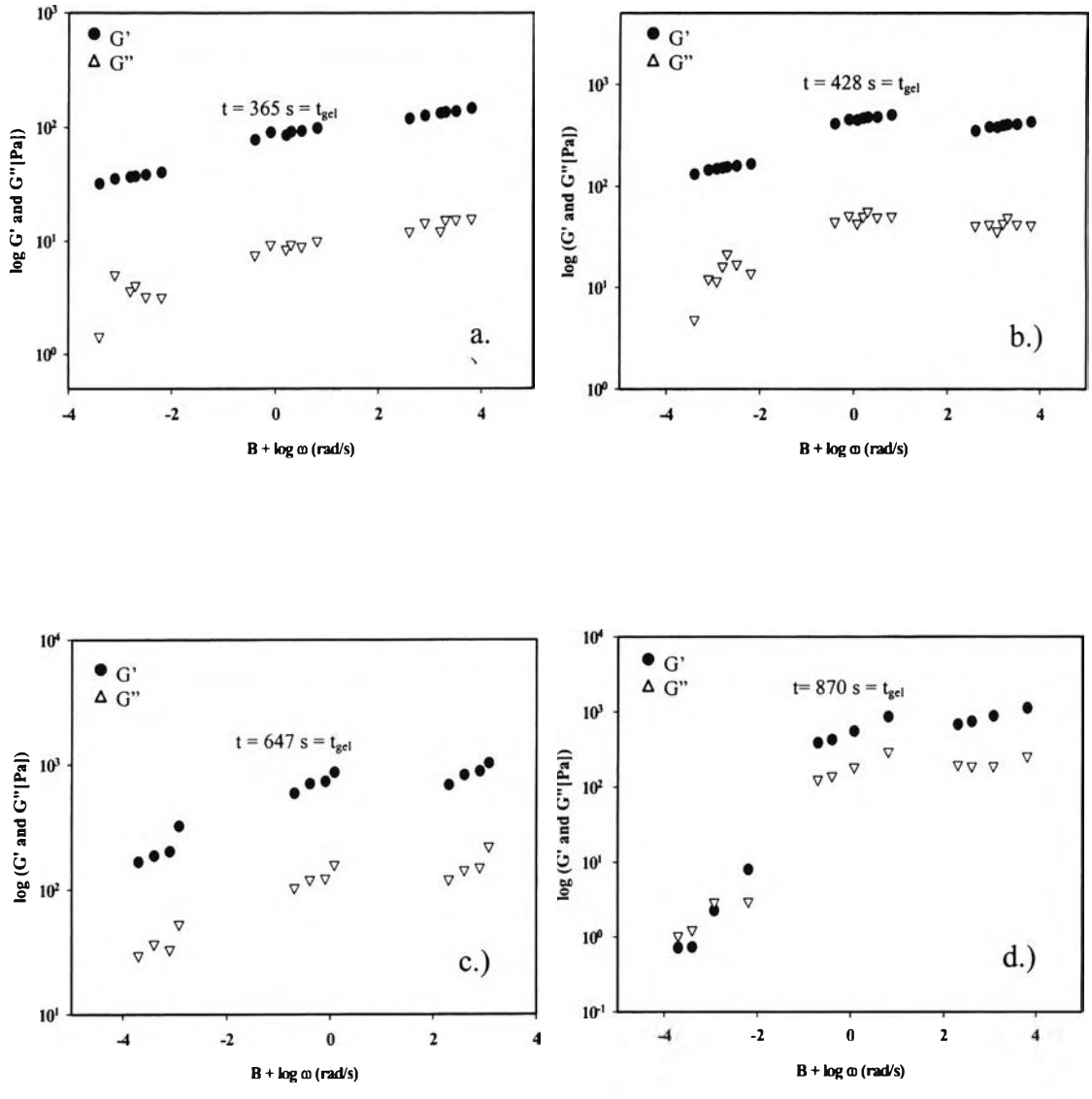

Figure 5.9 The frequency dependence curves of G' (ω) and G" (ω) at (λ) pregel stage(B = -3),(ν) gel point,and (B = 0),and (σ) postgel stage (B = 3) of a.) 0.28, b.) 0.33, c.) 0.39 and d.) 0.45 HCl:H_2O ratio.

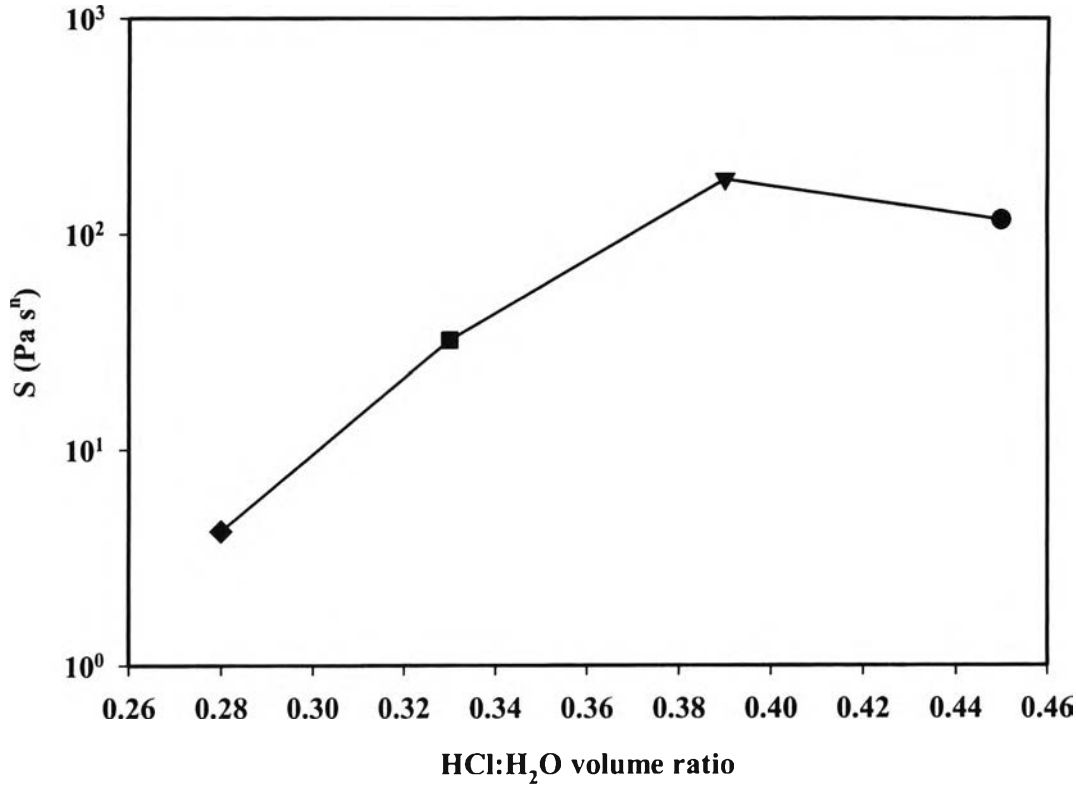

Figure 5.10 The plot of gel strength parameter S at the gel point as a function of $HCl:H_2O$ volume ratio : 0.28 (◆), 0.33 (■), 0.39(▲) and 0.45 (●).

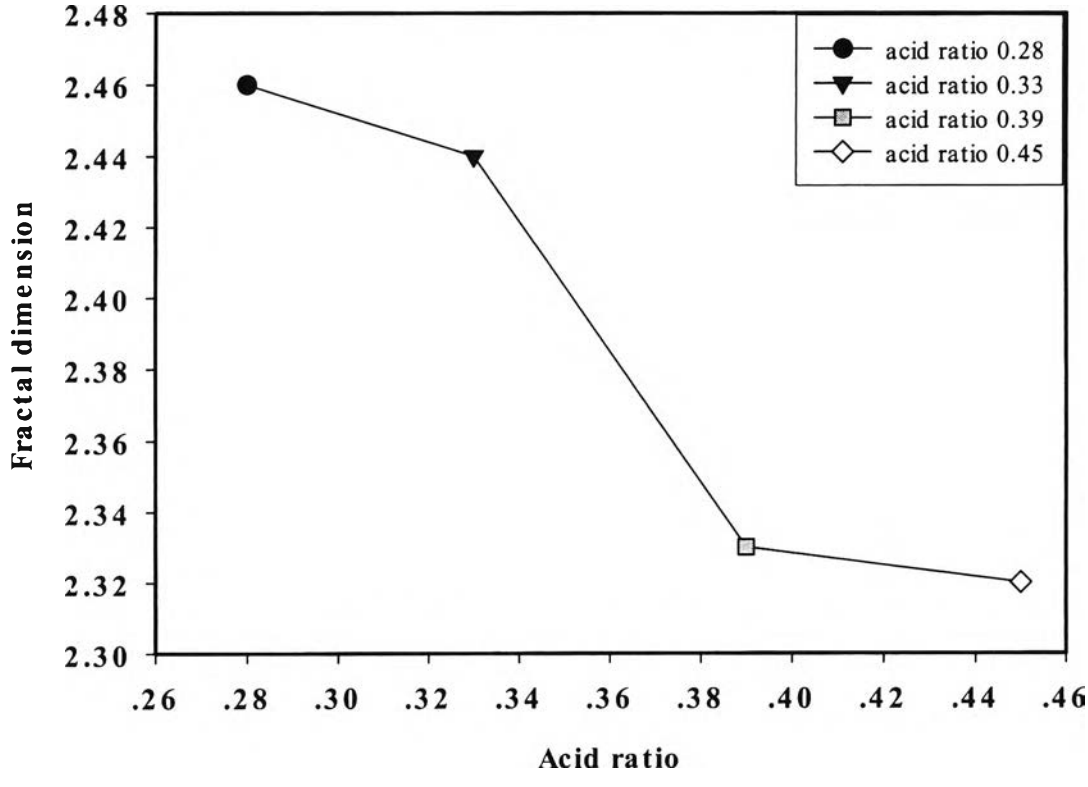

Figure 5.11 The plot of fractal dimension of the critical gel ccluster as a function of acid ratio.

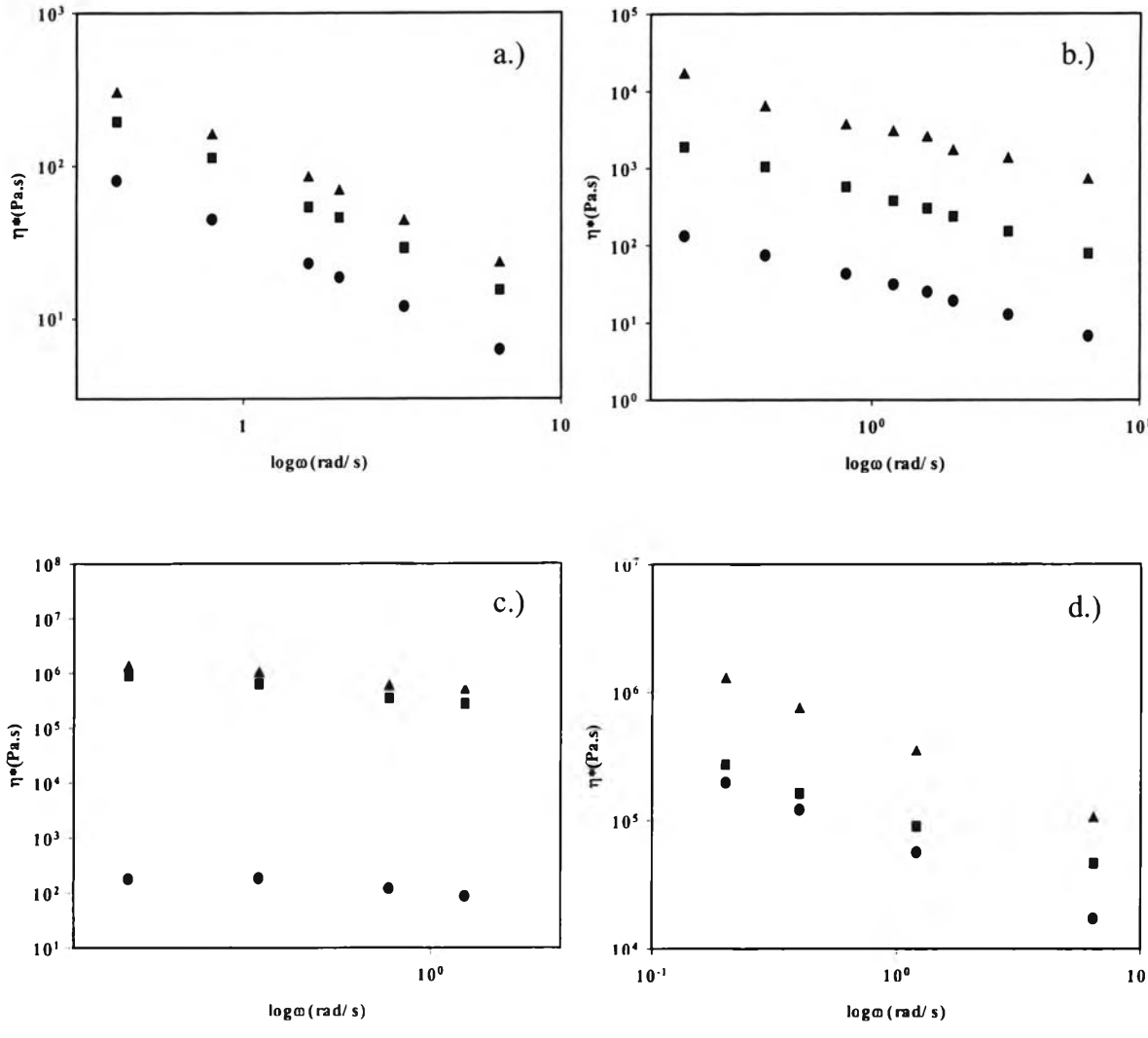

Figure 5.12 The effect of frequency on the complex viscosity at pregel stage, gel point, and postgel stage of a.) 0.28, b.) 0.33, c.) 0.39 and d.) 0.45 HCl:H_2O volume ratio.

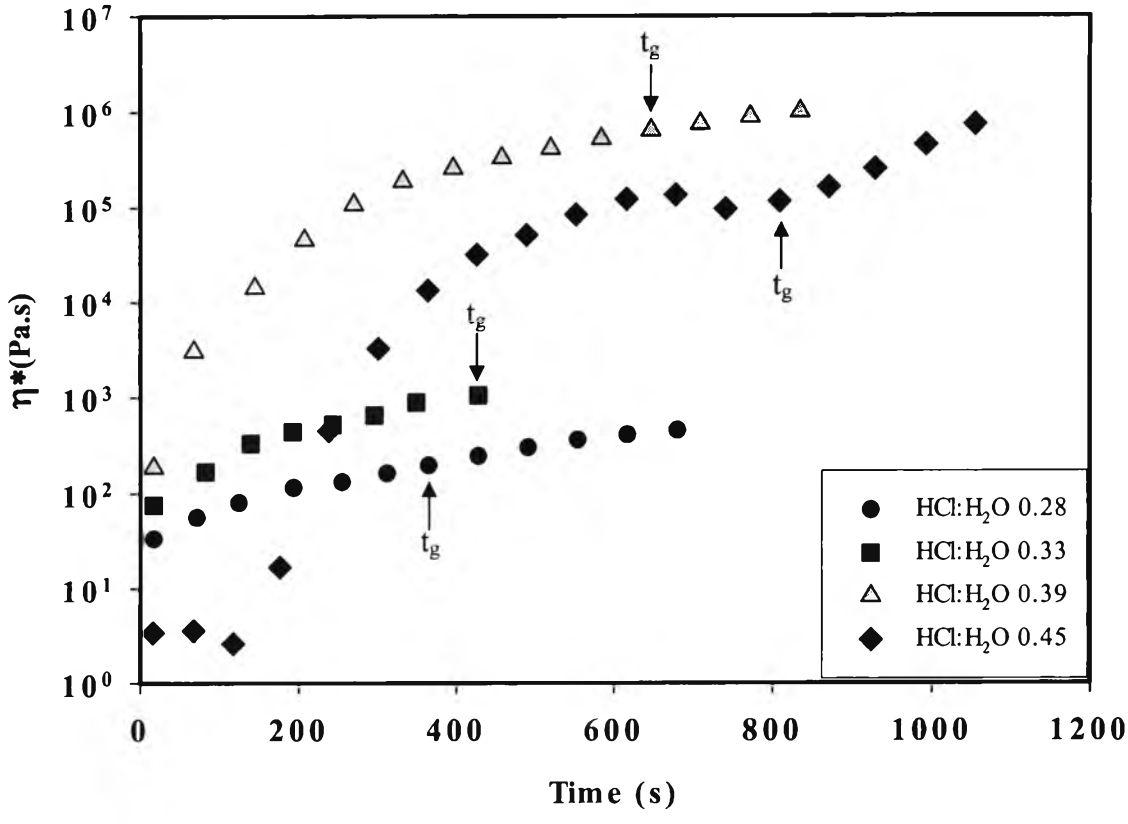

Figure 5.13 The time evolution of the complex viscosity (at fixed frequency of 0.4 rad/s) of a.) 0.28, b.) 0.33, c.) 0.39 and d.) 0.45 HCl:H_2O volume ratio.